Available online at www.sciencedirect.com
ScienceDirect
Ceramics International 37 (2011) 3045–3048
CERAMICS INTERNATIONAL
www.elsevier.com/locate/ceramint

Microstructural, electrical and magnetic properties of multiferroic $CoFe_2O_4$/0.68Pb($Mg_{1/3}Nb_{2/3}$)O_3–0.32$PbTiO_3$ nanocomposite thin films

M. Feng [a,b], W. Wang [a,*], J.C. Rao [a], Y. Zhou [a], D.C. Jia [a], H.B. Li [b]

[a] Institute for Advanced Ceramics, Department of Materials Science, Harbin Institute of Technology, Harbin 150001, PR China
[b] Key Laboratory of Functional Materials Physics and Chemistry of the Ministry of Education, Jilin Normal University, Siping 136000, PR China

Received 12 March 2011; received in revised form 3 May 2011; accepted 5 May 2011
Available online 12 May 2011

Abstract

Bilayered $CoFe_2O_4$/0.68Pb($Mg_{1/3}Nb_{2/3}$)O_3–0.32$PbTiO_3$ nanocomposite films are successfully prepared on Pt/Ti/SiO_2/Si substrate via simple sol–gel process. X-ray diffraction result reveals that there exists no chemical reaction or phase diffusion between the $CoFe_2O_4$ and 0.68Pb($Mg_{1/3}Nb_{2/3}$)O_3–0.32$PbTiO_3$ phases. The microstructure is characterized by scanning/transmission electron microscopy (STEM). The composite thin films exhibit both strong ferroelectric and ferromagnetic responses at room temperature. The maximal magnetoelectric coupling coefficient of the nanocomposite films reaches up to 25 mV/cm Oe, occurs at a lower bias magnetic field (H_{dc}) of 550 Oe.

Keywords: A. Sol–gel processes; B. Nanocomposites; C. Ferroelectric properties; Magnetoelectric coupling

1. Introduction

A great deal of investigation has been focused on multilayered and nanostructured ferroelectric/ferromagnetic thin films because of their potential applications in microsensors, actuators and new magnetic memories [1,2]. Such composite materials can display a spontaneous electric polarization as a response to an external magnetic field, or an induced magnetization by an applied electric field (i.e., a magnetoelectric (ME) effect). Some deposition techniques such as pulsed laser deposition [3], composition spreads [4], and sol–gel process [5] have been used to fabricate various magnetoelectric films. Of these techniques, sol–gel process is a versatile and inexpensive technique for producing multiferroic nanostructures, and particularly facilitates the fabrication of complex oxide films. So far, different 2-2-type combinations of ferromagnetic phase (e.g., $CoFe_2O_4$, $NiFe_2O_4$, and $La_{1-x}Sr_xMnO_3$) and ferroelectric phase (e.g., $PbZr_{1-x}Ti_xO_3$, $BaTiO_3$, $Bi_{4-x}La_xTi_3O_{12}$, and $BiFeO_3$) have been investigated by various experimental techniques [6–11]. However, to the best of our knowledge, experimental researches of CFO/PMN-PT composite thin films have been rarely reported.

In this work, composite multiferroic thin films consisting of top $CoFe_2O_4$ (CFO) layer and bottom 0.68Pb($Mg_{1/3}Nb_{2/3}$)O_3–0.32$PbTiO_3$ (PMN-PT) layer have been successfully grown on Pt/Ti/SiO_2/Si substrate via a simple sol–gel process. The microstructure of the cross-section sample was studied by scanning/transmission electron microscopy (STEM). The electrical, magnetic, and magnetoelectric properties were also investigated.

2. Experimental

Multiferroic CFO/PMN-PT 2-2 type bilayered films were prepared by a sol–gel process and spin-coating technique. Cobalt nitrate hexahydrate $Co(NO_3)_2{\cdot}6H_2O$ and iron nitrate nonahydrate $Fe(NO_3)_3{\cdot}9H_2O$ were dissolved in 2-methaoxyethanol to get a precursor solution of cobalt ferrite $CoFe_2O_4$. The PMN-PT precursor solution could be obtained via the sol–gel process as reported previously [12]. Firstly, the PMN-PT precursor solutions were spin coated on the Pt (1 1 1)/Ti/SiO_2/Si substrate at 4000 rpm for 30 s and pyrolyzed on a hot plate at 450 °C for 5 min. The pyrolyzed thin films were performed by repeating above processes to obtain a desired thickness, and finally annealed at 650 °C for 10 min by rapid thermal

* Corresponding author. Tel.: +86 451 86402040; fax: +86 451 86414291.
E-mail address: wangwen@hit.edu.cn (W. Wang).

0272-8842/$36.00
doi:10.1016/j.ceramint.2011.05.031

annealing (RTA). Secondly, the CFO precursor solutions were spin coated repeatedly on the PMN-PT layer until the CFO layer achieved a desired thickness via the same process. But the second step of the annealing process was performed to crystallize the CFO layer at 750 °C for 10 min by RTA.

The phase of the composite thin films and its orientation were analyzed by X-ray diffraction (XRD, Rigaku, D/max-2500/PC). The microstructure of the cross-section sample was also studied by scanning/transmission electron microscopy (STEM) equipped with a high-angle annular dark field (HAADF) detector (FEI, Tecnai G^2 F20) operating at 200 kV. The ferroelectric hysteresis loops of the composite thin films were measured by ferroelectric tester (Precision LC, Radiant Technologies). The magnetic measurements were performed with vibrating sample magnetometer (VSM, Lake Shore, M-7407). The ME coupling properties were measured by the applied alternating magnetic field (H) of 100 Oe over a prescribed frequency of 1 kHz under various dc bias magnetic fields (H_{dc}) of up to 6 kOe. The voltage signal generated from the films induced by the in-plane magnetic field was measured through a lock-in amplifier (SRS Inc., SR850, Sunnyvale, CA).

3. Results and discussion

Fig. 1 shows the XRD patterns of CFO/PMN-PT nanocomposite thin films rapidly heat-treated at 650 °C and then post heat-treated at temperature of 750 °C for 10 min. It is found that all the peaks corresponding to CFO and PMN-PT compositional phases. The PMN-PT layer was mainly crystallized to perovskite phase. However, a little trace of pyrochlore phase (at angles $2\theta = 29^\circ$ and 34°) was also detected. The layer exhibited a highly (1 1 1) preferred orientation when first pyrolyzed at 450 °C, and then annealed by the two-step process, of which the orientation controlling is the same as the single phase PMN-PT films. $CoFe_2O_4$ phases are polycrystalline structures and have no evident preferential crystallographic orientations. It was reported that the (1 1 1)-oriented PMN film

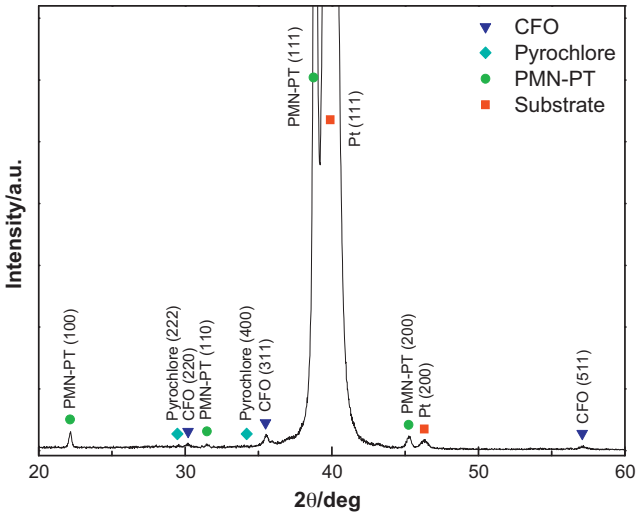

Fig. 1. XRD patterns of CFO/PMN-PT nanocomposite thin films.

was preferentially formed due to low interfacial energy, which resulted from the fact that the lattice parameters of Pt (1 1 1) crystal plane matched closely with those of PMN (1 1 1) [13]. The bottom PMN-PT layer of composite films has been completely crystallized before deposited the top CFO layer. Thus, the PMN-PT keeps the (1 1 1) preferential orientation unchanged after annealing at 750 °C for 10 min.

Fig. 2 shows cross-sectional bright-field TEM (a) and HAADF-STEM (b) images of the CFO/PMN-PT nanocomposite films grown on the Pt/Ti/SiO_2/Si substrate. The microstructure of different layers is obvious as well as the substrate. The interfaces between two layers are indicated by arrows. The tungsten (W) layer was coated to protect sample surface during FIB processing. These images clearly show that each layer was almost uniform in thickness and that all the interfaces were smooth. As shown in Fig. 2(a) and (b), the cross-sectional images clearly display the bilayered nanostructures, with a total thickness of ~325 nm. The bottom PMN-PT layer with (1 1 1)

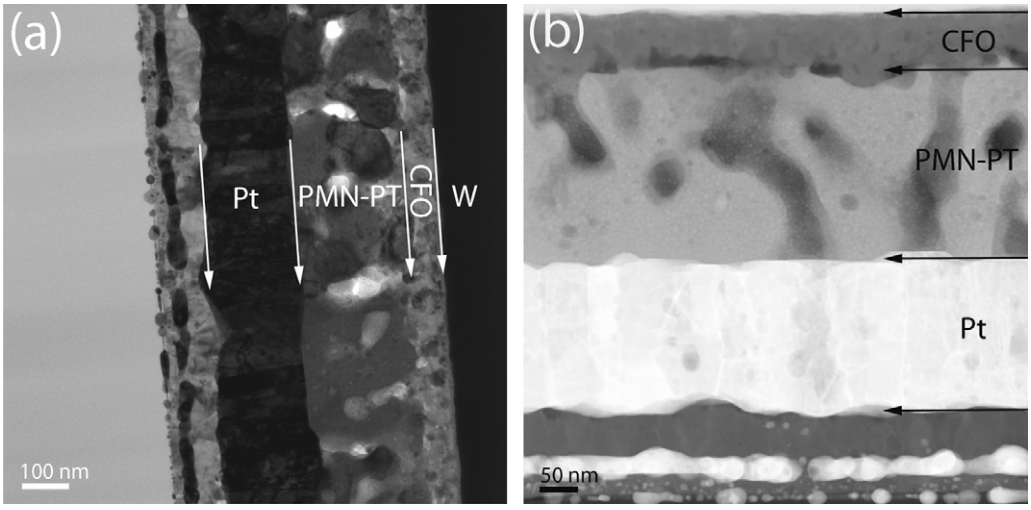

Fig. 2. Cross-sectional bright-field TEM (a) and HAADF-STEM (b) images of the CFO/PMN-PT nanocomposite films grown on the Pt/Ti/SiO_2/Si substrate. The interfaces between two layers are indicated by arrows.

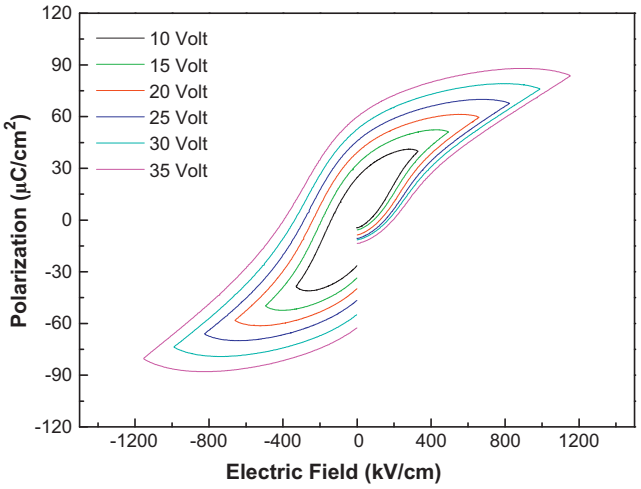

Fig. 3. Polarization vs. electric field (*P–E*) hysteresis loops for CFO/PMN-PT nanocomposite thin films with different applied voltages.

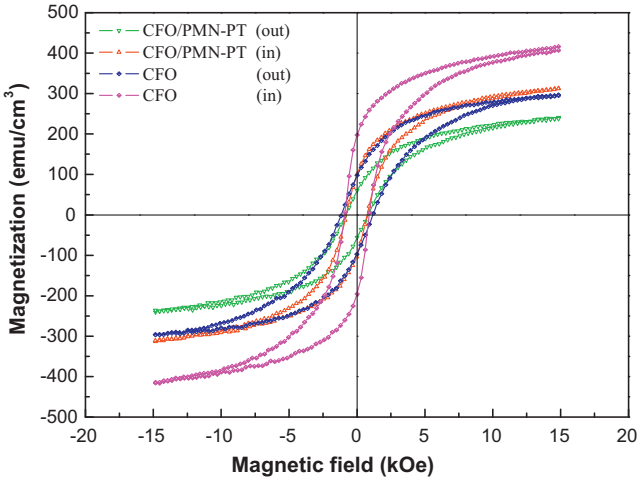

Fig. 4. In-plane and out-of plane magnetic hysteresis loops of the CFO/PMN-PT nanocomposite thin films. The hysteresis loops of the pure CFO thin films are also shown for comparison.

preferential orientation has a thickness of ~250 nm, while the CFO layer has a thickness of ~75 nm. The average atomic number of PMN-PT is larger than that of CFO, and thus in the HAADF-STEM images the PMN-PT layer appears lighter in contract than that of the CFO layer.

The polarization versus electric field (*P–E*) hysteresis loops under the applied voltage in the range of 10–35 V are shown in Fig. 3. The well-defined ferroelectric loops were observed in the nanocomposite thin films. The polarization and coercive field increase with increasing applied voltage. The remnant polarization P_r and saturated polarization P_s are 22.6 and 37.1 μC/cm^2 at an applied voltage of 10 V, respectively, for the nanocomposite thin film. Compared to the pure PMN-PT films described in Ref. [12], the composite films have higher coercivity (E_c = 80.8 kV/cm) because of the clamping effect resulted from the top CFO layer and the substrate during the switching of ferroelectric domains. Secondly, the CFO layer would cause lower effective voltage drop in the PMN-PT than the applied one, since the CFO layer of lower resistance also consumes some voltage [14]. Therefore, the coercivity of composite thin films is higher than that of the pure PMN-PT films.

Fig. 4 shows the typical magnetic hysteresis loops of the nanocomposite films which were measured with fields up to 15 kOe by applying magnetic fields parallel to the film plane (in plane) and perpendicular to the film plane (out of plane). The nanocomposite thin films demonstrated a much lower saturation magnetization (M_s) and coercivity (H_c) than the pure CFO thin film as shown in Fig. 4. Both the in-plane and out-of-plane loops have similar shapes, and the saturation magnetization of the in-plane and out-of-plane loops shows 293 and 236 emu/cm^3, respectively, which are lower than that of the pure $CoFe_2O_4$ films (M_s = 416 and 311 emu/cm^3). On the other hand, the coercivity H_c of the composite thin film is about 785 Oe and 860 Oe for both the in-plane and out-of-plane loops, much lower than that of the pure $CoFe_2O_4$ films (H_c = 927 and 1145 Oe). The in plane H_c is slightly smaller than the out of plane H_c while M_s is in reverse, which means the spins in-plane rotate relatively easily but are harder to saturate. This illustrates that the magnetic anisotropy in the composite thin film is evident. This shape anisotropy of the magnetic behavior is undoubtedly related to the CFO nanosheet structure that is oriented along in-plane directions. The saturation magnetizations are smaller than that of the pure CFO film, which should be ascribed to the compressive strains in the CFO phase caused by the lattice mismatch between the CFO and PMN-PT phases, leading to this easier magnetization characteristic due to the piezomagnetic effect [15].

The ME measurements were carried out by applying both constant (H_{dc}) and alternating (δ_H) magnetic fields parallel to the film plane. The change in the voltage increment δV induced by the in-plane dc bias magnetic field H_{dc} in the CFO/PMN-PT bilayered films is shown in Fig. 5. The ME response presents the trend of increases to its maximum at about 550 Oe and then decreases with increasing dc magnetic field H_{dc}. Our observation is in agreement with the bulk composite ceramics. The maximal ME coupling coefficient, defined as $\alpha_E = \delta V/\delta Ht$

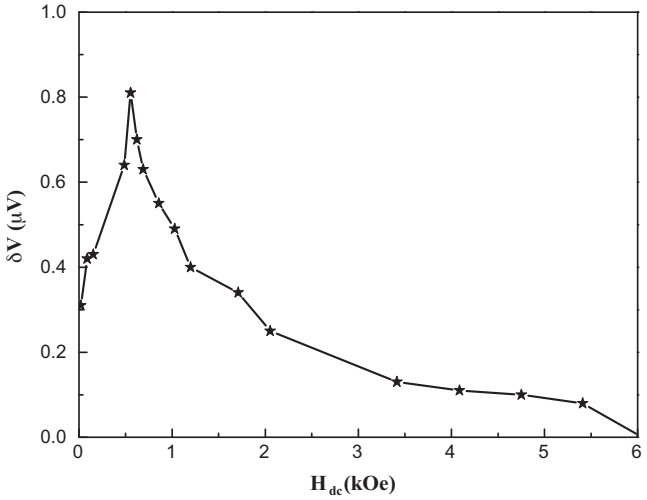

Fig. 5. Magnetically induced voltage increment δV as a function of dc bias magnetic field H_{dc} at 1 kHz for the CFO/PMN-PT bilayered thin films.

(t being the total thickness of the bilayered thin films), reaches up to about 25 mV/cm Oe, higher than that of the CFO/PZT bilayered films [14]. This result indicates that the CFO/PMN-PT nanocomposite film is a good candidate as a working material for ME random access memories and ME microsensor.

4. Conclusions

In summary, we have measured the ferroelectric and ferromagnetic response of CFO/PMN-PT nanocomposite thin films grown on Pt/Ti/SiO_2/Si substrate. X-ray diffraction analysis shows that all the peaks corresponding to CFO and PMN-PT compositional phases without the appearance of any additional or intermediate phase peaks. The PMN-PT phase in the multiferroic thin films was preferably oriented in the (1 1 1) orientation. HAADF-STEM image clearly shows that each layer was almost uniform in thickness and that all the interfaces were smooth. The nanocomposite thin films present strong coexistence of ferroelectric and ferromagnetic properties. The magnetically induced voltage increases to its maximum at about 550 Oe and then decreases with increasing dc bias magnetic field H_{dc}.

Acknowledgements

The authors would like to thank the financial support from National Natural Science Foundation of China with the project Nos. 50872024 and 51021002, NSFC-RFBR joint project No. 51011120099, and the Fundamental Research Funds for the Central Universities (Grant No. HIT.NSRIF.2009031).

References

[1] H. Zheng, J. Wang, S.E. Lofland, Z. Ma, L. Mohaddes-Ardabili, T. Zhao, L. Salamanca-Riba, S.R. Shinde, S.B. Ogale, F. Bai, D. Viehland, Y. Jia, D.G. Schlom, M. Wuttig, A. Roytburd, R. Ramesh, Multiferroic $BaTiO_3$–$CoFe_2O_4$ nanostructures, Science 303 (2004) 661–663.

[2] J. Wu, J. Wang, Multiferroic behavior of $BiFeO_3$–$RTiO_3$ (Mg, Sr, Ca, Ba, and Pb) thin films, J. Appl. Phys. 108 (2010) 026101.

[3] I. Levin, J. Li, J. Slutsker, A.L. Roytburd, Design of self-assembled multiferroic nanostructures in epitaxial films, Adv. Mater. 18 (2006) 2044–2047.

[4] K.S. Chang, M.A. Aronova, C.L. Lin, M. Murakami, M.H. Yu, J. Hattrick-Simpers, O.O. Famodu, S.Y. Lee, R. Ramesh, M. Wuttig, I. Takeuchi, C. Gao, L.A. Bendersky, Exploration of artificial multiferroic thin-film heterostructures using composition spreads, Appl. Phys. Lett. 84 (2004) 3091–3093.

[5] J.G. Wan, X.W. Wang, Y.J. Wu, M. Zeng, Y. Wang, H. Jiang, W.Q. Zhou, G.H. Wang, J.M. Liu, Magnetoelectric $CoFe_2O_4$–Pb(Zr, Ti)O_3 composite thin films derived by a sol–gel process, Appl. Phys. Lett. 86 (2005) 122501.

[6] C.Y. Deng, Y. Zhang, J. Ma, Y.H. Lin, C.W. Nan, Magnetoelectric effect in multiferroic heteroepitaxial $BaTiO_3$–$NiFe_2O_4$ composite thin films, Acta Mater. 56 (2008) 405–412.

[7] Y.G. Ma, W.N. Cheng, M. Ning, C.K. Ong, Magnetoelectric effect in epitaxial $Pb(Zr_{0.52}Ti_{0.48})O_3$/$La_{0.7}Sr_{0.3}MnO_3$ composite thin film, Appl. Phys. Lett. 90 (2007) 152911.

[8] C.C. Zhou, K.X. Jin, B.C. Luo, X.S. Cao, C.L. Chen, Photoconductivity in $BiFeO_3$/$La_{0.7}Sr_{0.3}MnO_3$ heterostructure, Mater. Lett. 64 (2010) 1713–1716.

[9] H.C. He, J.P. Zhou, J. Wang, C.W. Nan, Multiferroic $Pb(Zr_{0.52}Ti_{0.48})O_3$–$Co_{0.9}Zn_{0.1}Fe_2O_4$ bilayer thin films via a solution processing, Appl. Phys. Lett. 89 (2006) 052904.

[10] F.Z. Huang, X.M. Lu, W.W. Lin, W. Cai, X.M. Wu, Y. Kan, H. Sang, J.S. Zhu, Multiferroic properties and dielectric relaxation of $BiFeO_3$/$Bi_{3.25}La_{0.75}Ti_3O_{12}$ double-layered thin films, Appl. Phys. Lett. 90 (2007) 252903.

[11] C.H. Sim, Z.Z. Pan, J. Wang, Residual stress and magnetic behavior of multiferroic $CoFe_2O_4$/$Pb(Zr_{0.52}Ti_{0.48})O_3$ thin films, J. Appl. Phys. 105 (2009) 084113.

[12] M. Feng, W. Wang, H. Ke, J.C. Rao, Y. Zhou, Highly (1 1 1)-oriented and pyrochlore-free PMN-PT thin films derived from a modified sol–gel process, J. Alloys Compd. 495 (2010) 154–157.

[13] K. Okuwada, M. Imai, K. Kakuno, Preparation of $Pb(Mg_{1/3}Nb_{2/3})O_3$ thin film by sol–gel method, Jpn. J. Appl. Phys. Part 2 (28) (1989) L1271–1273.

[14] H.C. He, J. Ma, Y.H. Lin, C.W. Nan, Influence of relative thickness on multiferroic properties of bilayered $Pb(Zr_{0.52}Ti_{0.48})O_3$–$CoFe_2O_4$ thin films, J. Appl. Phys. 104 (2008) 114114.

[15] R.C. O'Handley, Modern Magnetic Materials: Principles and Applications, Wiley, New York, 2000.